Dynamical Systems in Neuroscience: The Geometry of Excitability and Bursting

Eugene M. Izhikevich

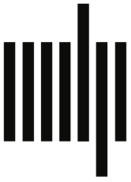

The MIT Press

From The MIT Press

MITCogNet

This book was set in LaTeX by the author. Printed and bound in the United States of America.

Library of Congress Cataloging-in-Publication Data

Izhikevich, Eugene M., 1967–
Dynamical systems in neuroscience: the geometry of excitability and bursting / Eugene M. Izhikevich.
p. cm. — (Computational neuroscience)
Includes bibliographical references and index.
ISBN 978-0-262-09043-8 (hc. : alk. paper)
1. Neural networks (Neurobiology) 2. Neurons - computer simulation. 3. Dynamical systems. 4. Computational neuroscience. I. Izhikevich, E. M. II Title. III. Series.

QP363.3.I94 2007
573.8'01'13—DC21 2006040349

10 9 8 7 6 5 4 3 2 1

Chapter 2

Electrophysiology of Neurons

In this chapter we remind the reader of some fundamental concepts of neuronal electrophysiology that are necessary to understand the rest of the book. We start with ions and currents, and move quickly toward the dynamics of the Hodgkin-Huxley model. If the reader is already familiar with the Hodgkin-Huxley formalism, this chapter can be skipped. Our exposition is brief, and it cannot substitute for a good introductory neuroscience course or the reading of such excellent textbooks as *Theoretical Neuroscience* by Dayan and Abbott (2001), *Foundations of Cellular Neurophysiology* by Johnston and Wu (1995), *Biophysics of Computation* by Koch (1999), or *Ion Channels of Excitable Membranes* by Hille (2001).

2.1 Ions

Electrical activity in neurons is sustained and propagated via ionic currents through neuron membranes. Most of these transmembrane currents involve one of four ionic species: sodium (Na^+), potassium (K^+), calcium (Ca^{2+}), or chloride (Cl^-). The first three have a positive charge (cations) and the fourth has a negative charge (anion). The concentrations of these ions are different on the inside and the outside of a cell, which creates electrochemical gradients – the major driving forces of neural activity. The extracellular medium has a high concentration of Na^+ and Cl^- (salty, like seawater) and a relatively high concentration of Ca^{2+}. The intracellular medium has high concentrations of K^+ and negatively charged molecules (denoted by A^-), as we illustrate in Fig.2.1.

The cell membrane has large protein molecules forming channels through which ions (but not A^-) can flow according to their electrochemical gradients. The flow of Na^+ and Ca^{2+} ions is not significant, at least at rest, but the flow of K^+ and Cl^- ions is. This, however, does not eliminate the concentration asymmetry for two reasons.

- *Passive redistribution.* The impermeable anions A^- attract more K^+ into the cell (opposites attract) and repel more Cl^- out of the cell, thereby creating concentration gradients.
- *Active transport.* Ions are pumped in and out of the cell via ionic pumps. For example, the Na^+-K^+ pump depicted in Fig.2.1 pumps out three Na^+ ions for every two K^+ ions pumped in, thereby maintaining concentration gradients.

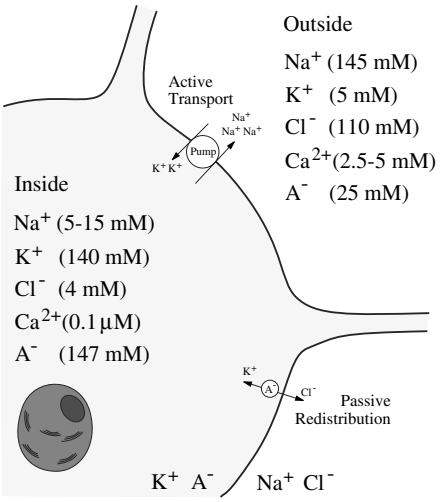

Equilibrium Potentials

$$\begin{aligned}
\mathrm{Na}^+ \quad & 62 \log \tfrac{145}{5} = 90 \text{ mV} \\
& 62 \log \tfrac{145}{15} = 61 \text{ mV} \\
\mathrm{K}^+ \quad & 62 \log \tfrac{5}{140} = -90 \text{ mV} \\
\mathrm{Cl}^- \quad & -62 \log \tfrac{110}{4} = -89 \text{ mV} \\
\mathrm{Ca}^{2+} \quad & 31 \log \tfrac{2.5}{10^{-4}} = 136 \text{ mV} \\
& 31 \log \tfrac{5}{10^{-4}} = 146 \text{ mV}
\end{aligned}$$

Figure 2.1: Ion concentrations and Nernst equilibrium potentials (2.1) in a typical mammalian neuron (modified from Johnston and Wu 1995). A^- are membrane-impermeant anions. Temperature $T = 37°\mathrm{C}$ (310°K).

2.1.1 Nernst Potential

There are two forces that drive each ion species through the membrane channel: concentration and electric potential gradients. First, the ions diffuse down the concentration gradient. For example, the K^+ ions depicted in Fig.2.2a diffuse out of the cell because K^+ concentration inside is higher than that outside. While exiting the cell, K^+ ions carry a positive charge and leave a net negative charge inside the cell (consisting mostly of impermeable anions A^-), thereby producing the outward current. The positive and negative charges accumulate on the opposite sides of the membrane surface, creating an electric potential gradient across the membrane – *transmembrane potential* or *membrane voltage*. This potential slows the diffusion of K^+, since K^+ ions are attracted to the negatively charged interior and repelled from the positively charged exterior of the membrane, as we illustrate in Fig.2.2b. At some point an equilibrium is achieved: the concentration gradient and the electric potential gradient exert equal and opposite forces that counterbalance each other, and the net cross-membrane current is zero, as in Fig.2.2c. The value of such an *equilibrium potential* depends on the ionic species, and it is given by the Nernst equation (Hille 2001):

$$E_{\text{ion}} = \frac{RT}{zF} \ln \frac{[\text{Ion}]_{\text{out}}}{[\text{Ion}]_{\text{in}}} , \tag{2.1}$$

where $[\text{Ion}]_{\text{in}}$ and $[\text{Ion}]_{\text{out}}$ are concentrations of the ions inside and outside the cell, respectively; R is the universal gas constant ($8,315$ mJ/(K°·Mol)); T is temperature in degrees Kelvin (K° = 273.16+C°); F is Faraday's constant ($96,480$ coulombs/Mol),

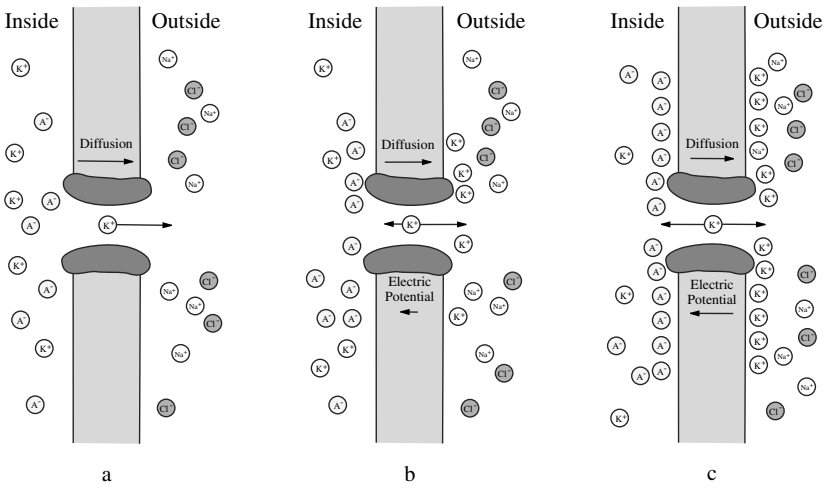

Figure 2.2: Diffusion of K^+ ions down the concentration gradient though the membrane (a) creates an electric potential force pointing in the opposite direction (b) until the diffusion and electrical forces counter each other (c). The resulting transmembrane potential (2.1) is referred to as the Nernst equilibrium potential for K^+.

z is the valence of the ion ($z = 1$ for Na^+ and K^+; $z = -1$ for Cl^-; and $z = 2$ for Ca^{2+}). Substituting the numbers, taking $\log_{10}$ instead of natural ln and using body temperature $T = 310°K$ (37°C) results in

$$E_{\text{ion}} \approx 62 \log \frac{[\text{Ion}]_{\text{out}}}{[\text{Ion}]_{\text{in}}} \quad (\text{mV})$$

for monovalent ($z = 1$) ions. Nernst equilibrium potentials in a typical mammalian neuron are summarized in Fig.2.1.

2.1.2 Ionic Currents and Conductances

In the rest of the book V denotes the membrane potential and E_{Na}, E_{Ca}, E_{K}, and E_{Cl} denote the Nernst equilibrium potentials. When the membrane potential equals the equilibrium potential, say E_{K}, the net K^+ current, denoted as I_{K} ($\mu A/cm^2$), is zero (this is the definition of the Nernst equilibrium potential for K^+). Otherwise, the net K^+ current is proportional to the difference of potentials; that is,

$$I_{\text{K}} = g_{\text{K}} (V - E_{\text{K}}) ,$$

where the positive parameter g_{K} (mS/cm^2) is the K^+ conductance and $(V - E_{\text{K}})$ is the K^+ *driving force.* The other major ionic currents,

$$I_{\text{Na}} = g_{\text{Na}} (V - E_{\text{Na}}) , \qquad I_{\text{Ca}} = g_{\text{Ca}} (V - E_{\text{Ca}}) , \qquad I_{\text{Cl}} = g_{\text{Cl}} (V - E_{\text{Cl}}) ,$$

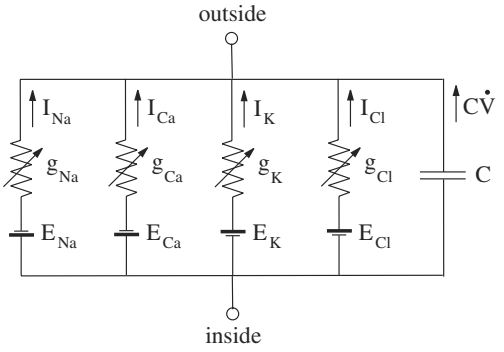

Figure 2.3: Equivalent circuit representation of a patch of cell membrane.

could also be expressed as products of nonlinear conductances and corresponding driving forces. A better description of membrane currents, especially Ca^{2+} current, is provided by the Goldman-Hodgkin-Katz equation (Hille 2001), which we do not use in this book.

When the conductance is constant, the current is said to be *Ohmic*. In general, ionic currents in neurons are not Ohmic, since the conductances may depend on time, membrane potential, and pharmacological agents, e.g., neurotransmitters, neuromodulators, second-messengers, etc. It is the time-dependent variation in conductances that allows a neuron to generate an action potential, or spike.

2.1.3 Equivalent Circuit

It is traditional to represent electrical properties of membranes in terms of equivalent circuits similar to the one depicted in Fig.2.3. According to Kirchhoff's law, the total current, I, flowing across a patch of a cell membrane is the sum of the membrane capacitive current $C\dot{V}$ (the capacitance $C \approx 1.0\,\mu\mathrm{F/cm^2}$ in the squid axon) and all the ionic currents

$$I = C\dot{V} + I_{\mathrm{Na}} + I_{\mathrm{Ca}} + I_{\mathrm{K}} + I_{\mathrm{Cl}} \,,$$

where $\dot{V} = dV/dt$ is the derivative of the voltage variable V with respect to time t. The derivative arises because it takes time to charge the membrane. This is the first *dynamic* term in the book! We write this equation in the standard "dynamical system" form

$$C\dot{V} = I - I_{\mathrm{Na}} - I_{\mathrm{Ca}} - I_{\mathrm{K}} - I_{\mathrm{Cl}} \tag{2.2}$$

or

$$C\dot{V} = I - g_{\mathrm{Na}}\,(V - E_{\mathrm{Na}}) - g_{\mathrm{Ca}}\,(V - E_{\mathrm{Ca}}) - g_{\mathrm{K}}\,(V - E_{\mathrm{K}}) - g_{\mathrm{Cl}}\,(V - E_{\mathrm{Cl}}) \,. \tag{2.3}$$

If there are no additional current sources or sinks, such as synaptic current, axial current, or tangential current along the membrane surface, or current injected via an

electrode, then $I = 0$. In this case, the membrane potential is typically bounded by the equilibrium potentials in the order (see Fig.2.4)

$$E_{\rm K} < E_{\rm Cl} < V_{\rm (at\ rest)} < E_{\rm Na} < E_{\rm Ca}\ ,$$

so that $I_{\rm Na}, I_{\rm Ca} < 0$ (inward currents) and $I_{\rm K}, I_{\rm Cl} > 0$ (outward currents). From (2.2) it follows that inward currents increase the membrane potential, that is, make it more positive (depolarization), whereas outward currents decrease it, that is, make it more negative (hyperpolarization). Note that $I_{\rm Cl}$ is called an outward current even though the flow of Cl^- ions is inward; the ions bring negative charge inside the membrane, which is equivalent to positively charged ions leaving the cell, as in $I_{\rm K}$.

2.1.4 Resting Potential and Input Resistance

If there were only K^+ channels, as in Fig.2.2, the membrane potential would quickly approach the K^+ equilibrium potential, $E_{\rm K}$, which is around -90 mV. Indeed,

$$C\,\dot{V} = -I_{\rm K} = -g_{\rm K}(V - E_{\rm K})$$

in this case. However, most membranes contain a diversity of channels. For example, Na^+ channels would produce an inward current and pull the membrane potential toward the Na^+ equilibrium potential, $E_{\rm Na}$, which could be as large as $+90$ mV. The value of the membrane potential at which all inward and outward currents balance each other so that the net membrane current is zero corresponds to the *resting membrane potential*. It can be found from (2.3) with $I = 0$, by setting $\dot{V} = 0$. The resulting expression,

$$V_{\rm rest} = \frac{g_{\rm Na}E_{\rm Na} + g_{\rm Ca}E_{\rm Ca} + g_{\rm K}E_{\rm K} + g_{\rm Cl}E_{\rm Cl}}{g_{\rm Na} + g_{\rm Ca} + g_{\rm K} + g_{\rm Cl}} \tag{2.4}$$

has a nice mechanistic interpretation: $V_{\rm rest}$ is the center of mass of the balance depicted in Fig.2.4. Incidentally, the entire equation (2.3) can be written in the form

$$C\,\dot{V} = I - g_{\rm inp}(V - V_{\rm rest})\ , \tag{2.5}$$

where

$$g_{\rm inp} = g_{\rm Na} + g_{\rm Ca} + g_{\rm K} + g_{\rm Cl}$$

is the total membrane conductance, called *input conductance*. The quantity $R_{\rm inp} = 1/g_{\rm inp}$ is the *input resistance* of the membrane, and it measures the asymptotic sensitivity of the membrane potential to injected or intrinsic currents. Indeed, from (2.5) it follows that

$$V \to V_{\rm rest} + IR_{\rm inp}\ , \tag{2.6}$$

so greater values of $R_{\rm inp}$ imply greater steady-state displacement of V due to the injection of DC current I.

A remarkable property of neuronal membranes is that ionic conductances, and hence the input resistance, are functions of V and time. We can use (2.6) to trace an action

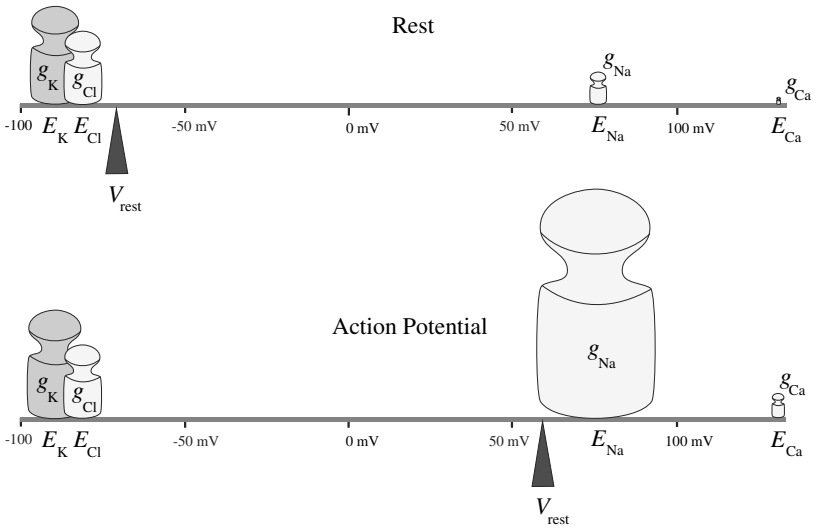

Figure 2.4: Mechanistic interpretation of the resting membrane potential (2.4) as the center of mass. Na^+ conductance increases during the action potential.

potential in a quasi-static fashion, i.e., assuming that time is frozen. When a neuron is quiescent, Na^+ and Ca^{2+} conductances are relatively small, V_{rest} is near E_{K} and E_{Cl}, as in Fig.2.4 (top), and so is V. During the upstroke of an action potential, the Na^+ or Ca^{2+} conductance becomes very large; V_{rest} is near E_{Na}, as in Fig.2.4 (bottom), and V increases, trying to catch V_{rest}. This event is, however, quite brief, for the reasons explained in subsequent sections.

2.1.5 Voltage-Clamp and I-V Relation

In section 2.2 we will study how the membrane potential affects ionic conductances and currents, assuming that the potential is fixed at certain value V_{c} controlled by an experimenter. To maintain the membrane potential constant (clamped), one inserts a metallic conductor to short-circuit currents along the membrane (space-clamp), and then injects a current proportional to the difference $V_{\text{c}} - V$ (voltage-clamp), as in Fig.2.5. From (2.2) and the clamp condition $\dot{V} = 0$, it follows that the injected current I equals the net current generated by the membrane conductances.

In a typical voltage-clamp experiment the membrane potential is held at a certain resting value V_{c} and then reset to a new value V_{s}, as in Fig.2.6a. The injected membrane current needed to stabilize the potential at the new value is a function of time, the pre-step holding potential V_{c}, and the step potential V_{s}. First, the current jumps to a new value to accommodate the instantaneous voltage change from V_{c} to V_{s}. From (2.5) we find that the amplitude of the jump is $g_{\text{inp}}(V_{\text{s}} - V_{\text{c}})$. Then, time- and voltage-

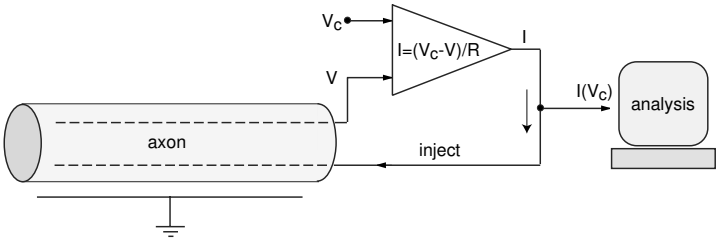

Figure 2.5: Two-wire voltage-clamp experiment on the axon. The top wire is used to monitor the membrane potential V. The bottom wire is used to inject the current I, proportional to the difference $V_c - V$, to keep the membrane potential at V_c.

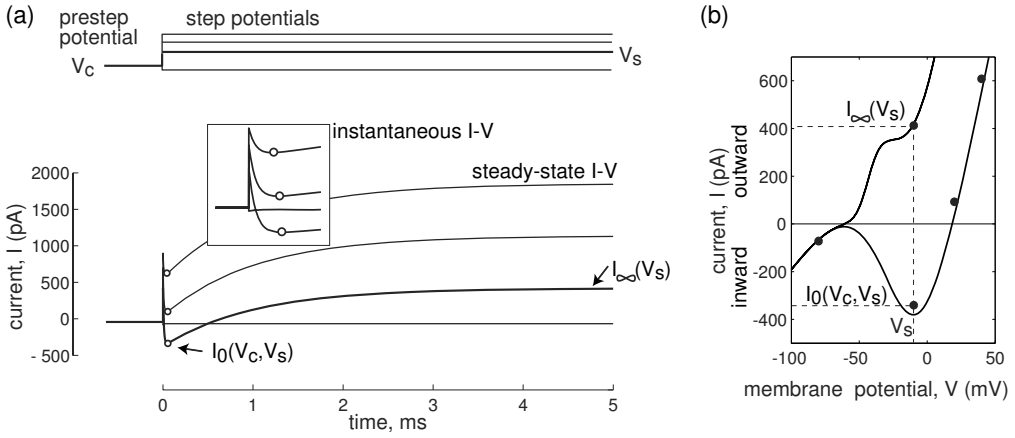

Figure 2.6: Voltage-clamp experiment to measure instantaneous and steady-state I-V relation. Shown are simulations of the $I_{\rm Na}$+$I_{\rm K}$-model (see Fig.4.1b); the continuous curves are theoretically found I-V relations.

dependent processes start to occur and the current decreases and then increases. The value at the negative peak, marked by the open circle "o" in Fig.2.6, depends only on V_c and V_s, and it is called *the instantaneous current-voltage (I-V) relation*, or $I_0(V_c, V_s)$. The asymptotic ($t \to \infty$) value depends only on V_s and it is called the *steady-state current-voltage (I-V) relation*, or $I_\infty(V_s)$.

Both relations, depicted in Fig.2.6b, can be found experimentally (black circles) or theoretically (curves). The instantaneous I-V relation usually has a non-monotone N-shape reflecting nonlinear autocatalytic (positive feedback) transmembrane processes, which are fast enough on the time scale of the action potential that they can be assumed to have instantaneous kinetics. The steady-state I-V relation measures the asymptotic values of all transmembrane processes, and it may be monotone (as in the figure) or not, depending on the properties of the membrane currents. Both I-V relations provide invaluable quantitative information about the currents operating on fast and slow time

Figure 2.7: To tease out neuronal currents, biologists employ an arsenal of sophisticated "clamp" methods, such as current-, voltage-, conductance-, and dynamic-clamp.

scales, and both are useful in building mathematical models of neurons. Finally, when $I_\infty(V) = 0$, the net membrane current is zero, and the potential is at rest or equilibrium, which may still be unstable, as we discuss in the next chapter.

2.2 Conductances

Ionic channels are large transmembrane proteins having aqueous pores through which ions can flow down their electrochemical gradients. The electrical conductance of individual channels may be controlled by gating particles (gates), which switch the channels between open and closed states. The gates may be sensitive to the following factors:

- *Membrane potential.* Example: voltage-gated Na^+ or K^+ channels
- *Intracellular agents* (second-messengers). Example: Ca^{2+}-gated K^+ channels
- *Extracellular agents* (neurotransmitters and neuromodulators). Examples: AMPA, NMDA, or GABA receptors.

Despite the stochastic nature of transitions between open and closed states in individual channels, the net current generated by a large population or ensemble of identical channels can reasonably be described by the equation

$$I = \bar{g}\, p\, (V - E)\ , \tag{2.7}$$

where p is the average proportion of channels in the open state, $\bar{g}$ is the *maximal conductance* of the population, and E is the *reverse potential* of the current, i.e., the potential at which the current reverses its direction. If the channels are selective

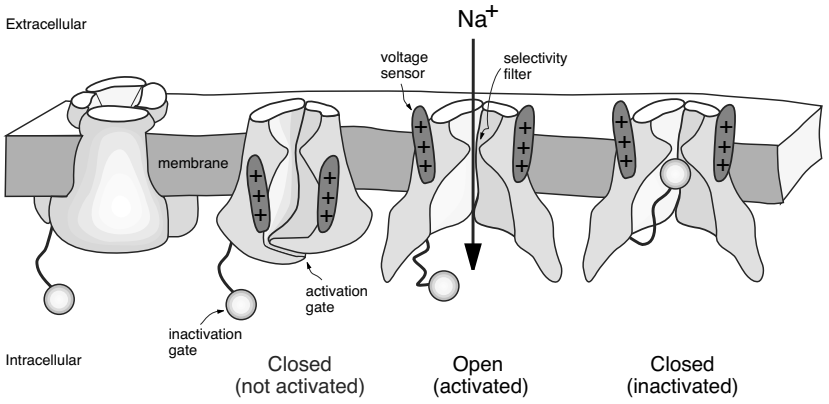

Figure 2.8: Structure of voltage-gated ion channels. Voltage sensors open an activation gate and allow selected ions to flow through the channel according to their electrochemical gradients. The inactivation gate blocks the channel. (Modified from Armstrong and Hille 1998.)

for a single ionic species, then the reverse potential E equals the Nernst equilibrium potential (2.1) for that ionic species (see exercise 2).

2.2.1 Voltage-Gated Channels

When the gating particles are sensitive to the membrane potential, the channels are said to be *voltage-gated*. The gates are divided into two types: those that *activate* or open the channels, and those that *inactivate* or close them (see Fig.2.8). According to the tradition initiated in the middle of the twentieth century by Hodgkin and Huxley, the probability of an activation gate being in the open state is denoted by the variable m (sometimes the variable n is used for K^+ and Cl^- channels). The probability of an inactivation gate being in the open state is denoted by the variable h. The proportion of open channels in a large population is

$$p = m^a \, h^b \, , \tag{2.8}$$

where a is the number of activation gates and b is the number of inactivation gates per channel. The channels can be partially ($0 < m < 1$) or completely *activated* ($m = 1$); not activated or *deactivated* ($m = 0$); *inactivated* ($h = 0$); released from inactivation or *deinactivated* ($h = 1$). Some channels do not have inactivation gates ($b = 0$), hence $p = m^a$. Such channels do not inactivate, and they result in *persistent* currents. In contrast, channels that do inactivate result in *transient* currents.

Below we describe voltage- and time-dependent kinetics of gates. This description is often referred to as the *Hodgkin-Huxley gate model* of membrane channels.

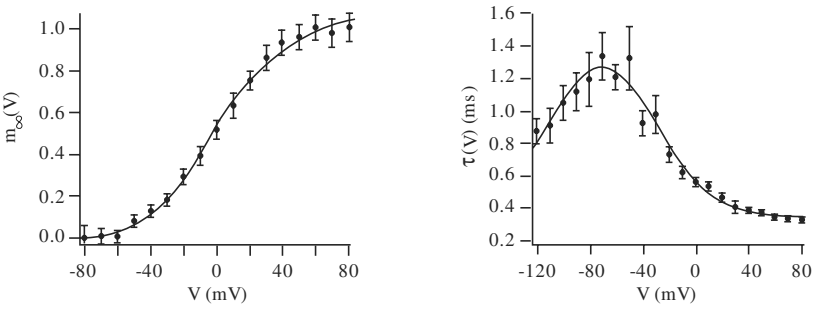

Figure 2.9: The activation function $m_\infty(V)$ and the time constant $\tau(V)$ of the fast transient K^+ current in layer 5 neocortical pyramidal neurons. (Modified from Korngreen and Sakmann 2000.)

2.2.2 Activation of Persistent Currents

The dynamics of the activation variable m is described by the first-order differential equation

$$\dot{m} = (m_\infty(V) - m)/\tau(V) \,, \tag{2.9}$$

where the voltage-sensitive steady-state *activation function* $m_\infty(V)$ and the *time constant* $\tau(V)$ can be measured experimentally. They have sigmoid and unimodal shapes, respectively, as in Fig.2.9 (see also Fig.2.20). The steady-state activation function $m_\infty(V)$ gives the asymptotic value of m when the potential is fixed (voltage-clamp). Smaller values of $\tau(V)$ result in faster dynamics of m.

In Fig.2.10 we depict a typical experiment to determine $m_\infty(V)$ of a persistent current, i.e., a current having no inactivation variable. Initially we hold the membrane potential at a hyperpolarized value V_0 so that all activation gates are closed and $I \approx 0$. Then we step-increase V to a greater value V_s ($s = 1, \ldots, 7$; see Fig.2.10a) and hold it there until the current is essentially equal to its asymptotic value, which is denoted here as I_s (s stands for "step"; see Fig.2.10b). Repeating the experiment for various stepping potentials V_s, one can easily determine the corresponding I_s, and hence the entire steady-state I-V relation, which we depict in Fig.2.10c. According to (2.7), $I(V) = \bar{g} m_\infty(V)(V - E)$, and the steady-state activation curve $m_\infty(V)$ depicted in Fig.2.10d is $I(V)$ divided by the driving force $(V - E)$ and normalized so that $\max m_\infty(V) = 1$. To determine the time constant $\tau(V)$, one needs to analyze the convergence rates. In exercise 6 we describe an efficient method to determine $m_\infty(V)$ and $\tau(V)$.

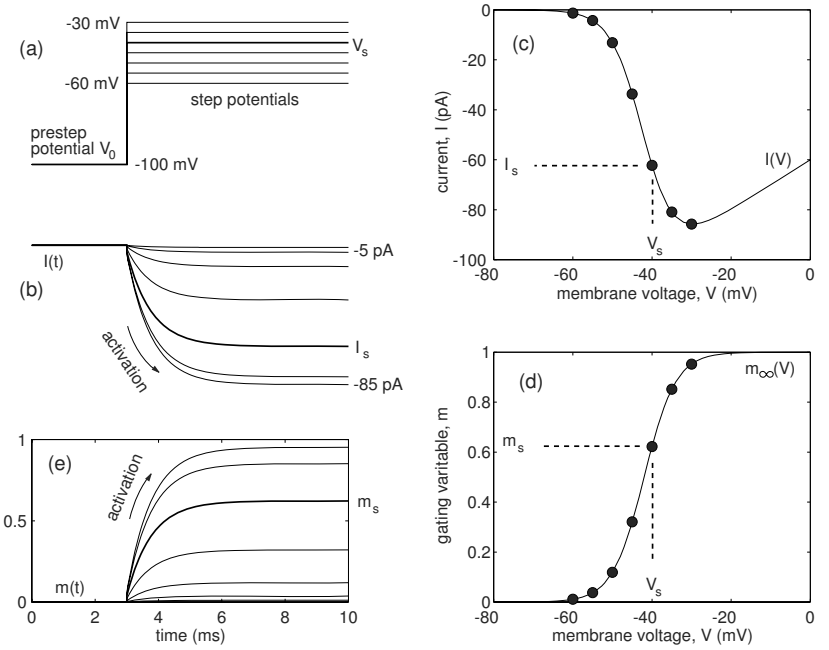

Figure 2.10: An experiment to determine $m_\infty(V)$. Shown are simulations of the persistent Na^+ current in Purkinje cells (see section 2.3.5).

2.2.3 Inactivation of Transient Currents

The dynamics of the inactivation variable h can be described by the first-order differential equation

$$\dot{h} = (h_\infty(V) - h)/\tau(V) \;, \tag{2.10}$$

where $h_\infty(V)$ is the voltage-sensitive steady-state *inactivation function* depicted in Fig.2.11. In Fig.2.12 we present a typical voltage-clamp experiment to determine $h_\infty(V)$ in the presence of activation $m_\infty(V)$. It relies on the observation that inactivation kinetics is usually slower than activation kinetics. First, we hold the membrane potential at a certain pre-step potential V_s for a long enough time that the activation and inactivation variables are essentially equal to their steady-state values $m_\infty(V_s)$ and $h_\infty(V_s)$, respectively, which have yet to be determined. Then we step-increase V to a sufficiently high value V_0, chosen so that $m_\infty(V_0) \approx 1$. If activation is much faster than inactivation, m approaches 1 after the first few milliseconds, while h continues to be near its asymptotic value $h_s = h_\infty(V_s)$, which can be found from the peak value of the current $I_s \approx \bar{g} \cdot 1 \cdot h_s(V_s - E)$. Repeating this experiment for various pre-step potentials, one can determine the steady-state inactivation curve $h_\infty(V)$ in Fig.2.11. In exercise 6 we describe a better method to determine $h_\infty(V)$ that does not rely on the difference between the activation and inactivation time scales.

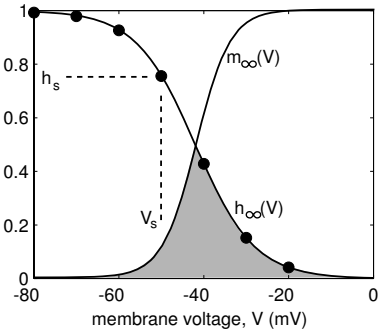

Figure 2.11: Steady-state activation function $m_\infty(V)$ from Fig.2.10, and inactivation function $h_\infty(V)$ and values h_s from Fig.2.12. Their overlap (shaded region) produces a noticeable, persistent "window" current.

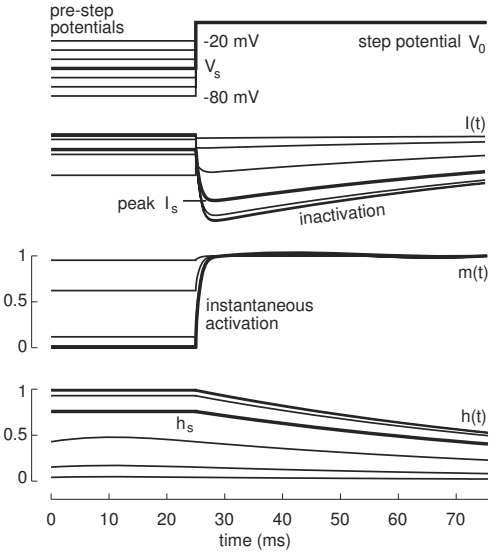

Figure 2.12: Dynamics of the current (I), activation (m), and inactivation (h) variables in the voltage-clamp experiment aimed at measuring $h_\infty(V)$ in Fig.2.11.

The voltage-sensitive steady-state activation and inactivation functions overlap in a shaded window depicted in Fig.2.11. Depending on the size of the shaded area in the figure, the overlap may result in a noticeable "window" current.

2.2.4 Hyperpolarization-Activated Channels

Many neurons in various parts of the brain have channels that are opened by hyperpolarization. These channels produce currents that are turned on by hyperpolarization and turned off by depolarization. Biologists refer to such currents as "exceptional" or "weird", and denote them as $I_{\rm Q}$ (queer), $I_{\rm f}$ (funny), $I_{\rm h}$ (hyperpolarization-activated), or $I_{\rm Kir}$ (K^+ inward rectifier). (We will consider the last two currents in detail in the next chapter). Most neuroscience textbooks classify these currents in a special category – *hyperpolarization-activated currents*. However, from the theoretical point of view, it is inconvenient to create special categories. In this book we treat these currents as

"normal" transient currents with the understanding that they are always activated (either $a = 0$ or variable $m = 1$ in (2.8)), but can be inactivated by depolarization (variable $h \to 0$) or deinactivated by hyperpolarization (variable $h \to 1$). Moreover, there is biophysical evidence suggesting that closing/opening of I_{Kir} is indeed related to the inactivation/deinactivation process (Lopatin et al. 1994).

2.3 The Hodgkin-Huxley Model

In section 2.1 we studied how the membrane potential depends on the membrane currents, assuming that ionic conductances are fixed. In section 2.2 we used the Hodgkin-Huxley gate model to study how the conductances and currents depend on the membrane potential, assuming that the potential is clamped at different values. In this section we put it all together and study how the potential $\leftrightarrow$ current nonlinear interactions lead to many interesting phenomena, such as generation of action potentials.

2.3.1 Hodgkin-Huxley Equations

One of the most important models in computational neuroscience is the Hodgkin-Huxley model of the squid giant axon. Using pioneering experimental techniques of that time, Hodgkin and Huxley (1952) determined that the squid axon carries three major currents: voltage-gated persistent K^+ current with four activation gates (resulting in the term n^4 in the equation below, where n is the activation variable for K^+); voltage-gated transient Na^+ current with three activation gates and one inactivation gate (the term m^3h below), and Ohmic leak current, I_{L}, which is carried mostly by Cl^- ions. The complete set of space-clamped Hodgkin-Huxley equations is

$$\begin{aligned} C\dot{V} &= I - \overbrace{\bar{g}_{\text{K}} n^4 (V - E_{\text{K}})}^{I_{\text{K}}} - \overbrace{\bar{g}_{\text{Na}} m^3 h (V - E_{\text{Na}})}^{I_{\text{Na}}} - \overbrace{g_{\text{L}} (V - E_{\text{L}})}^{I_{\text{L}}} \\ \dot{n} &= \alpha_n(V)(1-n) - \beta_n(V) n \\ \dot{m} &= \alpha_m(V)(1-m) - \beta_m(V) m \\ \dot{h} &= \alpha_h(V)(1-h) - \beta_h(V) h \,, \end{aligned}$$

where

$$\begin{aligned} \alpha_n(V) &= 0.01 \frac{10 - V}{\exp(\frac{10-V}{10}) - 1} \,, \\ \beta_n(V) &= 0.125 \exp\left(\frac{-V}{80}\right) \,, \\ \alpha_m(V) &= 0.1 \frac{25 - V}{\exp(\frac{25-V}{10}) - 1} \,, \\ \beta_m(V) &= 4 \exp\left(\frac{-V}{18}\right) \,, \end{aligned}$$

$$\begin{aligned} \alpha_h(V) &= 0.07 \exp\left(\frac{-V}{20}\right) , \\ \beta_h(V) &= \frac{1}{\exp(\frac{30-V}{10}) + 1} . \end{aligned}$$

These parameters, provided in the original Hodgkin and Huxley paper, correspond to the membrane potential shifted by approximately 65 mV, so that the resting potential is at $V \approx 0$. Hodgkin and Huxley did that for the sake of convenience, but the shift has led to a lot of confusion over the years. The shifted Nernst equilibrium potentials are

$$E_{\rm K} = -12 \text{ mV} , \qquad E_{\rm Na} = 120 \text{ mV} , \qquad E_{\rm L} = 10.6 \text{ mV};$$

(see also exercise 1). Typical values of maximal conductances are

$$\bar{g}_{\rm K} = 36 \text{ mS/cm}^2 , \qquad \bar{g}_{\rm Na} = 120 \text{ mS/cm}^2 , \qquad g_{\rm L} = 0.3 \text{ mS/cm}^2.$$

$C = 1\,\mu\text{F/cm}^2$ is the membrane capacitance and $I = 0\,\mu\text{A/cm}^2$ is the applied current. The functions $\alpha(V)$ and $\beta(V)$ describe the transition rates between open and closed states of the channels. We present this notation only for historical reasons. In the rest of the book, we use the standard form

$$\begin{aligned} \dot{n} &= (n_\infty(V) - n)/\tau_n(V) , \\ \dot{m} &= (m_\infty(V) - m)/\tau_m(V) , \\ \dot{h} &= (h_\infty(V) - h)/\tau_h(V) , \end{aligned}$$

where

$$\begin{aligned} n_\infty &= \alpha_n/(\alpha_n + \beta_n) , & \tau_n &= 1/(\alpha_n + \beta_n) , \\ m_\infty &= \alpha_m/(\alpha_m + \beta_m) , & \tau_m &= 1/(\alpha_m + \beta_m) , \\ h_\infty &= \alpha_h/(\alpha_h + \beta_h) , & \tau_h &= 1/(\alpha_h + \beta_h) \end{aligned}$$

as depicted in Fig.2.13. These functions can be approximated by the Boltzmann and Gaussian functions; see Ex. 4. We also shift the membrane potential back to its true value, so that the resting state is near -65 mV.

The membrane of the squid giant axon carries only two major currents: transient Na^+ and persistent K^+. Most neurons in the central nervous system have additional currents with diverse activation and inactivation dynamics, which we summarize in section 2.3.5. The Hodgkin-Huxley formalism is the most accepted model to describe their kinetics.

Since we are interested in geometrical and qualitative methods of analysis of neuronal models, we assume that all variables and parameters have appropriate scales and dimensions, but we do not explicitly state them. An exception is the membrane potential V, whose mV scale is stated in every figure.

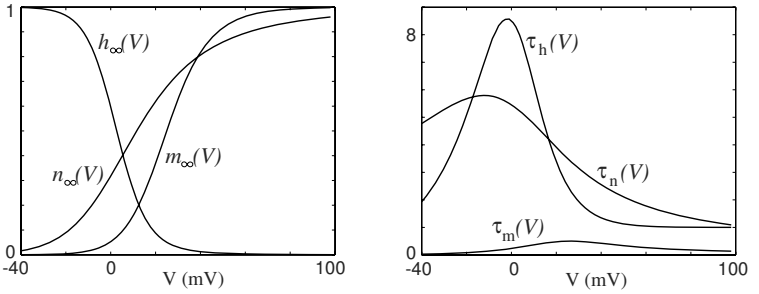

Figure 2.13: Steady-state (in)activation functions (left) and voltage-dependent time constants (right) in the Hodgkin-Huxley model.

Figure 2.14: Studies of spike-generation mechanism in "giant squid" axons won Alan Hodgkin and Andrew Huxley the 1963 Nobel Prize for physiology or medicine (shared with John Eccles). See also Fig. 4.1 in Keener and Sneyd (1998).

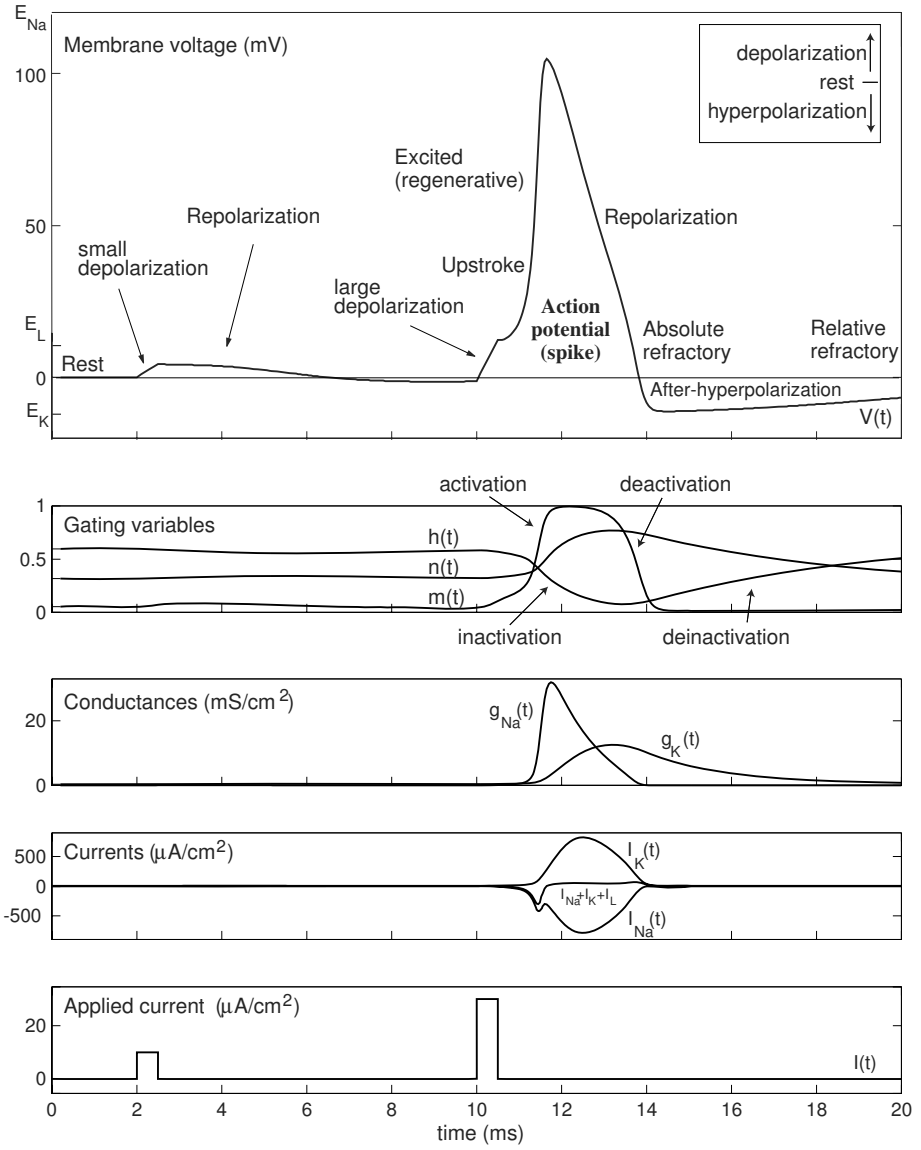

Figure 2.15: Action potential in the Hodgkin-Huxley model.

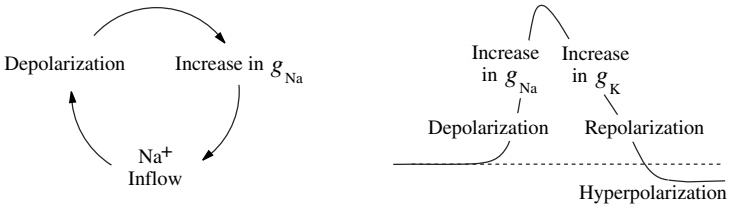

Figure 2.16: Positive and negative feedback loops resulting in excited (regenerative) behavior in neurons.

2.3.2 Action Potential

Recall that when $V = V_{\text{rest}}$, which is 0 mV in the Hodgkin-Huxley model, all inward and outward currents balance each other so the net current is zero, as in Fig.2.15. The resting state is stable: a small pulse of current applied via $I(t)$ produces a small positive perturbation of the membrane potential (depolarization), which results in a small net current that drives V back to resting (repolarization). However, an intermediate size pulse of current produces a perturbation that is amplified significantly because membrane conductances depend on V. Such a nonlinear amplification causes V to deviate considerably from V_{rest} – a phenomenon referred to as an *action potential* or *spike*.

In Fig.2.15 we show a typical time course of an action potential in the Hodgkin-Huxley system. Strong depolarization increases activation variables m and n and decreases inactivation variable h. Since $\tau_m(V)$ is relatively small, variable m is relatively fast. Fast activation of Na^+ conductance drives V toward E_{Na}, resulting in further depolarization and further activation of g_{Na}. This positive feedback loop, depicted in Fig.2.16, results in the *upstroke* of V. While V moves toward E_{Na}, the slower gating variables catch up. Variable $h \to 0$, causing inactivation of the Na^+ current, and variable $n \to 1$, causing slow activation of the outward K^+ current. The latter and the leak current repolarize the membrane potential toward V_{rest}.

When V is near V_{rest}, the voltage-sensitive time constants $\tau_{\text{n}}(V)$ and $\tau_{\text{h}}(V)$ are relatively large, as one can see in Fig.2.13. Therefore, recovery of variables n and h is slow. In particular, the outward K^+ current continues to be activated (n is large) even after the action potential downstroke, thereby causing V to go below V_{rest} toward E_{K} – a phenomenon known as *afterhyperpolarization*.

In addition, the Na^+ current continues to be inactivated (h is small) and not available for any regenerative function. The Hodgkin-Huxley system cannot generate another action potential during this *absolute refractory* period. While the current deinactivates, the system becomes able to generate an action potential, provided the stimulus is relatively strong (*relative refractory* period).

To study the relationship between these refractory periods, we stimulate the Hodgkin-Huxley model with 1-ms pulses of current having various amplitudes and latencies. The

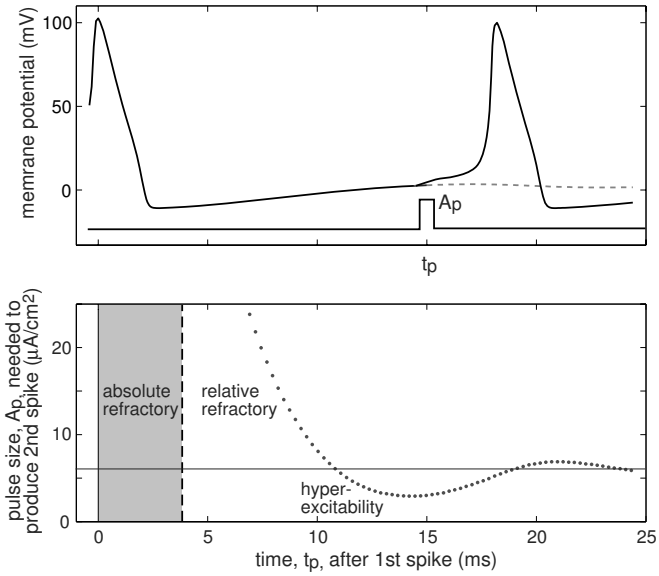

Figure 2.17: Refractory periods in the Hodgkin-Huxley model with $I = 3$.

minimal amplitude of the stimulation needed to evoke a second spike in the model is depicted in Fig.2.17 (bottom). Notice that around 14 ms after the first spike, the model is hyper-excitable, that is, the stimulation amplitude is less than the baseline amplitude $A_p \approx 6$ needed to evoke a spike from the resting state. This occurs because the Hodgkin-Huxley model exhibits damped oscillations of membrane potential (discussed in chapter 7).

2.3.3 Propagation of the Action Potentials

The space-clamped Hodgkin-Huxley model of the squid giant axon describes non-propagating action potentials since $V(t)$ does not depend on the location, x, along the axon. To describe propagation of action potentials (pulses) along the axon having potential $V(x,t)$, radius a (cm), and intracellular resistivity R (Ω·cm), the partial derivative V_{xx} is added to the voltage equation to account for axial currents along the membrane. The resulting nonlinear parabolic partial differential equation

$$C\,V_t = \frac{a}{2R}\,V_{xx} + I - I_{\rm K} - I_{\rm Na} - I_{\rm L}$$

is often referred to as the Hodgkin-Huxley cable or propagating equation. Its important type of solution, a traveling pulse, is depicted in Fig.2.18. Studying this equation goes beyond the scope of this book; the reader can consult Keener and Sneyd (1998) and references therein.

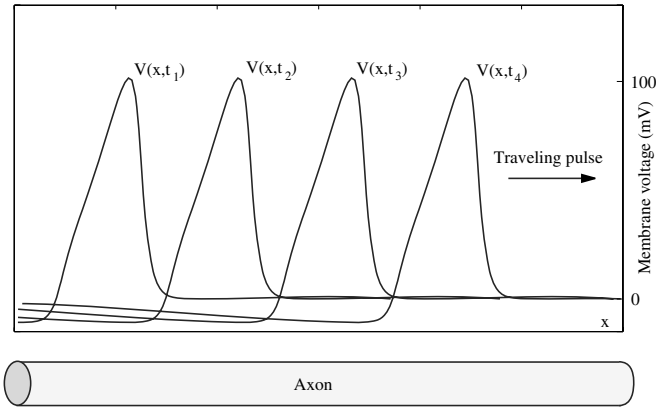

Figure 2.18: Traveling pulse solution of the Hodgkin-Huxley cable equation at four successive moments.

2.3.4 Dendritic Compartments

Modifications of the Hodgkin-Huxley model, often called Hodgkin-Huxley-type models or conductance-based models, can describe the dynamics of spike-generation of many, if not all, neurons recorded in nature. However, there is more to the computational property of neurons than just the spike-generation mechanism. Many neurons have an extensive dendritic tree that can sample the synaptic input arriving at different locations and integrate it over space and time.

Many dendrites have voltage-gated currents, so the synaptic integration is non-linear, sometimes resulting in dendritic spikes that can propagate forward to the soma of the neuron or backward to distant dendritic locations. Dendritic spikes are prominent in intrinsically bursting (IB) and chattering (CH) neocortical neurons considered in chapter 8. In that chapter we also model regular spiking (RS) pyramidal neurons, the most numerous class of neurons in mammalian neocortex, and show that their spike-generation mechanism is one of the simplest. The computation complexity of RS neurons must be hidden, then, in the arbors of their dendritic trees.

It is not feasible at present to study the dynamics of membrane potential in dendritic trees either analytically or geometrically (i.e., without resort to computer simulations), unless dendrites are assumed to be passive (linear) and semi-infinite, and to satisfy Rall's branching law (Rall 1959). Much of the insight can be obtained via simulations, which typically replace the continuous dendritic structure in Fig.2.19a with a network of discrete compartments in Fig.2.19b. Dynamics of each compartment is simulated by a Hodgkin-Huxley-type model, and the compartments are coupled via conductances. For example, if V_s and V_d denote the membrane potential at the soma and in the dendritic tree, respectively, as in Fig.2.19c, then

$$C_s\dot{V}_s = -I_s(V_s,t) + g_s(V_d - V_s)\ , \qquad \text{and} \qquad C_d\dot{V}_d = -I_d(V_d,t) + g_d(V_s - V_d)\ ,$$

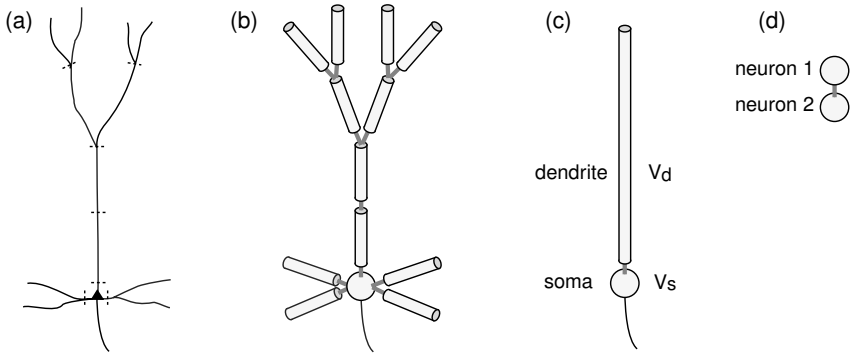

Figure 2.19: A dendritic tree of a neuron (a) is replaced by a network of compartments (b), each modeled by a Hodgkin-Huxley-type model. The two-compartment neuronal model (c) may be equivalent to two neurons coupled via gap junctions (electrical synapse) (d).

where each $I(V,t)$ represents the sum of all voltage-, Ca^{2+}-, and time-dependent currents in the compartment, and g_s and g_d are the coupling conductances that depend on the relative sizes of dendritic and somatic compartments. One can obtain many spiking and bursting patterns by changing the conductances and keeping all the other parameters fixed (Pinsky and Rinzel 1994, Mainen and Sejnowski 1996).

Once we understand how to couple two compartments, we can do it for hundreds or thousands of compartments. GENESIS and NEURON simulation environments could be useful here, especially since they contain databases of dendritic trees reconstructed from real neurons.

Interestingly, the somatic-dendritic pair in Fig.2.19c is equivalent to a pair of neurons in Fig.2.19d coupled via *gap-junctions*. These are electrical contacts that allow ions and small molecules to pass freely between the cells. Gap junctions are often called electrical synapses, because they allow potentials to be conducted directly from one neuron to another.

Computational study of multi-compartment dendritic processing is outside of the scope of this book. We consider multi-compartment models of cortical pyramidal neurons in chapter 8 and gap-junction coupled neurons in chapter 10 (which is on the author's webpage).

2.3.5 Summary of Voltage-Gated Currents

Throughout this book we model kinetics of various voltage-sensitive currents using the Hodgkin-Huxley gate model

$$I = \bar{g}\, m^a h^b (V - E)$$

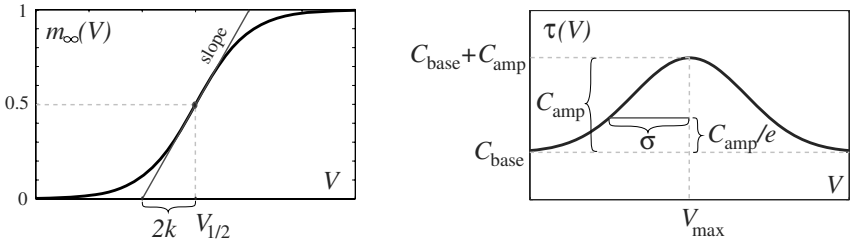

Figure 2.20: Boltzmann (2.11) and Gaussian (2.12) functions and geometrical interpretations of their parameters.

where
I - current , (μA/cm^2),
V - membrane voltage, (mV),
E - reverse potential, (mV),
$\bar{g}$ - maximal conductance, (mS/cm^2),
m - probability of activation gate to be open,
h - probability of inactivation gate to be open,
a - the number of activation gates per channel,
b - the number of inactivation gates per channel.
The gating variables m and n satisfy linear first-order differential equations (2.9) and (2.10), respectively. We approximate the steady-state activation curve $m_\infty(V)$ by the Boltzmann function depicted in Fig.2.20,

$$m_\infty(V) = \frac{1}{1 + \exp\{(V_{1/2} - V)/k\}} \tag{2.11}$$

The parameter $V_{1/2}$ satisfies $m_\infty(V_{1/2}) = 0.5$, and k is the slope factor (negative for the inactivation curve $h_\infty(V)$). Smaller values of $|k|$ result in steeper $m_\infty(V)$.

The voltage-sensitive time constant $\tau(V)$ can be approximated by the Gaussian function

$$\tau(V) = C_{\text{base}} + C_{\text{amp}} \exp \frac{-(V_{\max} - V)^2}{\sigma^2} , \tag{2.12}$$

see Fig.2.20. The graph of the function is above C_{base} with amplitude C_{amp}. The maximal value is achieved at $V_{\max}$. The parameter σ measures the characteristic width of the graph, that is, $\tau(V_{\max} \pm \sigma) = C_{\text{base}} + C_{\text{amp}}/e$. The Gaussian description is often not adequate, so we replace it with other functions whenever appropriate.

Below is the summary of voltage-gated currents whose kinetics were measured experimentally. The division into persistent and transient is somewhat artificial, since most "persistent" currents can still inactivate after seconds of prolonged depolarization. Hyperpolarization-activated currents, such as the h-current or K^+ inwardly rectifying current, are mathematically equivalent to currents that are always activated, but can be inactivated by depolarization. To avoid possible confusion, we mark these currents "opened by hyperpolarization".

Na^+ currents	Parameters (Fig.2.20) Eq. (2.11) $V_{1/2}$	k	Eq. (2.12) V_{max}	σ	C_{amp}	C_{base}
Fast transient [1]	$I_{Na,t} = \bar{g}\, m^3 h(V - E_{Na})$					
activation	−40	15	−38	30	0.46	0.04
inactivation	−62	−7	−67	20	7.4	1.2
Fast transient [2]	$I_{Na,t} = \bar{g}\, m_\infty(V) h(V - E_{Na})$					
activation	−30	5.5	–	–	–	–
inactivation	−70	−5.8	$\tau_h(V) = 3\exp((-40 - V)/33)$			
Fast transient [3]	$I_{Na,t} = \bar{g}\, m_\infty(V) h(V - E_{Na})$					
activation	−28	6.7	–	–	–	–
inactivation	−66	−6	$\tau_h(V) = 4\exp((-30 - V)/29)$			
Fast persistent [4,a]	$I_{Na,p} = \bar{g}\, m_\infty(V) h(V - E_{Na})$					
activation	−50	4	–	–	–	–
inactivation	−49	−10	−66	35	4.5 sec	2 sec
Fast persistent [5,a]	$I_{Na,p} = \bar{g}\, m_\infty(V)(0.14 + 0.86h)(V - E_{Na})$					
activation	−50	6	–	–	–	–
inactivation	−56	−7	$\tau_h(V) = 63.2 + 25\exp(-V/25.5)$			
Fast persistent [2]	$I_{Na,p} = \bar{g}\, m(V - E_{Na})$					
activation	−54	9	–	–	–	0.8
Fast persistent [6]	$I_{Na,p} = \bar{g}\, m(V - E_{Na})$					
activation	−42	4	–	–	–	0.8

1. Squid giant axon (Hodgkin and Huxley 1952); see exercise 4.
2. Thalamocortical neurons in rats (Parri and Crunelli 1999).
3. Thalamocortical neurons in cats (Parri and Crunelli 1999).
4. Layer-II principal neurons in entorhinal cortex (Magistretti and Alonso 1999).
5. Large dorsal root ganglion neurons in rats (Baker and Bostock 1997, 1998).
6. Purkinje cells (Kay et al. 1998).

a Very slow inactivation.

K^+ currents	Parameters (Fig.2.20) Eq. (2.11) $V_{1/2}$	k	Eq. (2.12) V_{max}	σ	C_{amp}	C_{base}
Delayed rectifier [1]	$I_K = \bar{g}\, n^4(V - E_K)$					
activation	−53	15	−79	50	4.7	1.1
Delayed rectifier [2,4]	$I_K = \bar{g}\, mh(V - E_K)$					
activation	−3	10	−50	30	47	5
inactivation	−51	−12	−50	50	1000	360
M current [3]	$I_{K(M)} = \bar{g}\, m(V - E_K)$					
activation	−44	8	−50	25	320	20
Transient [4]	$I_A = \bar{g}\, mh(V - E_K)$					
activation	−3	20	−71	60	0.92	0.34
inactivation	−66	−10	−73	23	50	8
Transient [5]	$I_A = \bar{g}\, mh(V - E_K)$					
activation	−26	20	–	–	–	–
inactivation	−72	−9.6	–	–	–	15.5
Transient [6]	$I_A = \bar{g}\, m^4 h\,(V - E_K)$					
Fast component (60% of total conductance)						
activation	−60	8.5	−58	25	2	0.37
inactivation	−78	−6	−78	25	45	19
Slow component (40% of total conductance)						
activation	−36	20	−58	25	2	0.37
inactivation	−78	−6	−78	25	45	19
			$\tau_h(V) = 60$ when $V > -73$			
Inward rectifier [7] (*opened by hyperpolarization*)	$I_{Kir} = \bar{g}\, h_\infty(V)(V - E_K)$					
inactivation	−80	−12	–	–	–	< 1

1. Squid giant axon (Hodgkin and Huxley 1952); see exercise 4.
2. Neocortical pyramidal neurons (Bekkers 2000).
3. Rodent neuroblastoma-glioma hybrid cells (Robbins et al. 1992).
4. Neocortical pyramidal neurons (Korngreen and Sakmann 2000).
5. Hippocampal mossy fiber boutons (Geiger and Jonas 2000).
6. Thalamic relay neurons (Huguenard and McCormick 1992).
7. Horizontal cells in catfish retina (Dong and Werblin 1995); AP cell of leech (Wessel et al. 1999); rat locus coeruleus neurons (Williams et al. 1988, $V_{1/2} = E_K$).

Cation currents	Parameters (Fig.2.20) Eq. (2.11) $V_{1/2}$	k	Eq. (2.12) $V_{\max}$	σ	C_{amp}	C_{base}
I_{h} current [1] ($\textit{opened by hyperpolarization}$)	$I_{\text{h}} = \bar{g}\, h\, (V - E_{\text{h}})$,		$E_{\text{h}} = -43$ mV			
inactivation	-75	-5.5	-75	15	1000	100
I_{h} current [2]	$I_{\text{h}} = \bar{g}\, h\, (V - E_{\text{h}})$,		$E_{\text{h}} = -1$ mV			
inact. (soma)	-82	-9	-75	20	50	10
inact. (dendrite)	-90	-8.5	-75	20	40	10
I_{h} current [3]	$I_{\text{h}} = \bar{g}\, h\, (V - E_{\text{h}})$,		$E_{\text{h}} = -21$ mV			
fast inact. (65%)	-67	-12	-75	30	50	20
slow inact. (35%)	-58	-9	-65	30	300	100

1. Thalamic relay neurons (McCormick and Pape 1990; Huguenard and McCormick 1992).
2. Hippocampal pyramidal neurons in CA1 (Magee 1998).
3. Entorhinal cortex layer II neurons (Dickson et al. 2000).

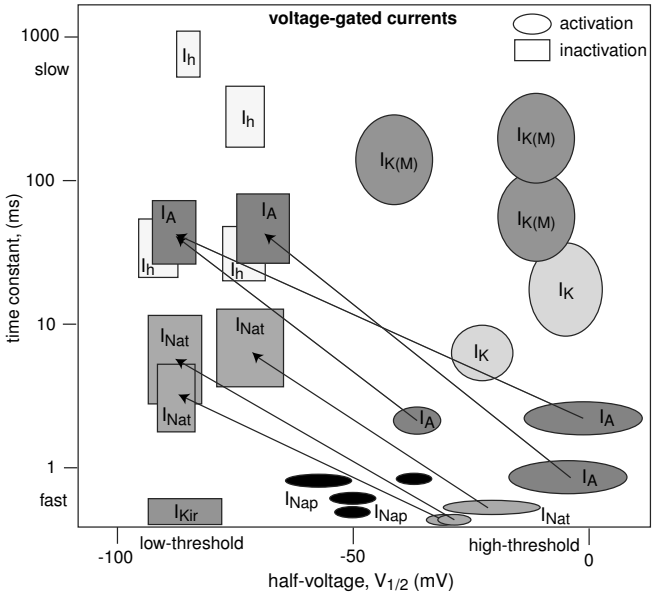

Figure 2.21: Summary of current kinetics. Each oval (rectangle) denotes the voltage and temporal scale of activation (inactivation) of a current. Transient currents are represented by arrows connecting ovals and rectangles.

Figure 2.22: Alan Hodgkin (right) and Andrew Huxley (left) in their Plymouth Marine Lab in 1949. (Photo provided by National Marine Biological Library, Plymouth, UK).

Review of Important Concepts

- Electrical signals in neurons are carried by Na^+, Ca^{2+}, K^+, and Cl^- ions, which move through membrane channels according to their electrochemical gradients.
- The membrane potential V is determined by the membrane conductances g_i and corresponding reversal potentials E_i:

$$C\,\dot{V} = I - \sum_i g_i \cdot (V - E_i)\ .$$

- Neurons are excitable because the conductances depend on the membrane potential and time.
- The most accepted description of kinetics of voltage-sensitive conductances is the Hodgkin-Huxley gate model.
- Voltage-gated activation of inward Na^+ or Ca^{2+} current depolarizes (increases) the membrane potential.
- Voltage-gated activation of outward K^+ or Cl^- current hyperpolarizes (decreases) the membrane potential.
- An action potential or spike is a brief regenerative depolarization of the membrane potential followed by its repolarization and possibly hyperpolarization, as in Fig.2.16.

Bibliographical Notes

Our summary of membrane electrophysiology is limited: we present only those concepts that are necessary to understand the Hodgkin-Huxley description of generation of action potentials. We have omitted such important topics as the Goldman-Hodgkin-Katz equation, cable theory, dendritic and synaptic function, although some of those will be introduced later in the book.

The standard textbook on membrane electrophysiology is the second edition of *Ion Channels of Excitable Membranes* by B. Hille (2001). An excellent introductory textbook with an emphasis on the quantitative approach is *Foundations of Cellular Neurophysiology* by D. Johnston and S. Wu (1995). A detailed introduction to mathematical aspects of cellular biophysics can be found in *Mathematical Physiology* by J. Keener and J. Sneyd (1998). The latter two books complement rather than repeat each other. *Biophysics of Computation* by Koch (1999) and chapters 5 and 6 of *Theoretical Neuroscience* by Dayan and Abbott (2001) provide a good introduction to biophysics of excitable membranes.

The first book devoted exclusively to dendrites is *Dendrites* by Stuart et al. (1999). It emphasizes the active nature of dendritic dynamics. Arshavsky et al. (1971; Russian language edition, 1969) make the first, and probably still the best, theoretical attempt to understand the neurocomputational properties of branching dendritic trees endowed with voltage-gated channels and capable of generating action potentials. Had they published their results in the 1990s, they would have been considered classics in the field. Unfortunately, the computational neuroscience community of the 1970s was not ready to accept the "heretic" idea that dendrites can fire spikes, that spikes can propagate backward and forward along the dendritic tree, that EPSPs can be scaled-up with distance, that individual dendritic branches can perform coincidence detection and branching points can perform nonlinear summation, and that different and independent computations can be carried out at different parts of the neuronal dendritic tree. We touch on some of these issues in chapter 8.

Exercises

1. Determine the Nernst equilibrium potentials for the membrane of the squid giant axon using the following data:

	Inside (mM)	Outside (mM)
K^+	430	20
Na^+	50	440
Cl^-	65	560

   and $T = 20°C$.

2. Show that a nonselective cation current

$$I = \bar{g}_{Na}\, p\, (V - E_{Na}) + \bar{g}_{K}\, p\, (V - E_{K})$$

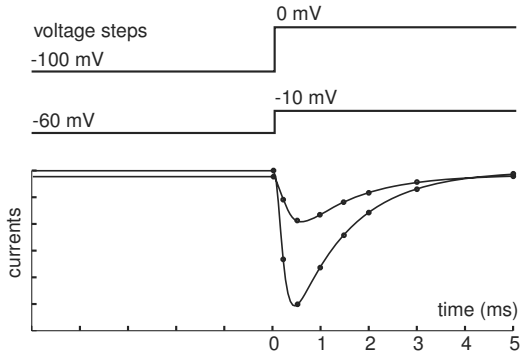

Figure 2.23: Current traces corresponding to voltage steps of various amplitudes; see exercise 6.

can be written in the form (2.7) with

$$\bar{g} = \bar{g}_{\rm Na} + \bar{g}_{\rm K} \qquad \text{and} \qquad E = \frac{\bar{g}_{\rm Na}E_{\rm Na} + \bar{g}_{\rm K}E_{\rm K}}{\bar{g}_{\rm Na} + \bar{g}_{\rm K}} \ .$$

3. Show that applying a DC current I in the neuronal model

$$C\dot{V} = I - g_{\rm L}(V - E_{\rm L}) - I_{\rm other}(V)$$

is equivalent to changing the leak reverse potential $E_{\rm L}$.

4. Steady-state (in)activation curves and voltage-sensitive time constants can be approximated by the Boltzmann (2.11) and Gaussian (2.12) functions, respectively, depicted in Fig.2.20. Explain the meaning of the parameters $V_{1/2}, k$, $C_{\rm base}, C_{\rm amp}, V_{\rm max}$, and σ and find their values that provide satisfactory fit near the rest state $V = 0$ for the Hodgkin-Huxley functions depicted in Fig.2.13.

5. (Willms et al. 1999) Consider the curve $m_\infty^p(V)$, where $m_\infty(V)$ is the Boltzmann function with parameters $V_{1/2}$ and k, and $p > 1$. This curve can be approximated by another Boltzmann function with some parameters $\tilde{V}_{1/2}$ and $\tilde{k}$ (and $p = 1$). Find the formulas that relate $\tilde{V}_{1/2}$ and $\tilde{k}$ to $V_{1/2}$, k, and p.

6. (Willms et al. 1999) Write a MATLAB program that determines activation and inactivation parameters via a simultaneous fitting of current traces from a voltage-clamp experiment similar to the one in Fig.2.23. Assume that the values of the voltage pairs – e.g., $-60, -10; -100, 0$ (mV) – are in the file `v.dat`. The values of the current (circles in Fig.2.23) are in the file `current.dat`, and the sampling times – e.g., 0, 0.25, 0.5, 1, 1.5, 2, 3, 5 (ms) – are in the file `times.dat`.

7. Modify the MATLAB program from exercise 6 to handle multi-step (Fig.2.24) and ramp protocols.

8. **[M.S.]** Find the best sequence of step potentials that can determine activation and inactivation parameters (a) in the shortest time, (b) with the highest precision.

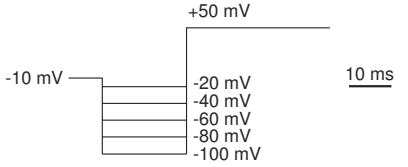

Figure 2.24: Multiple voltage steps are often needed to determine time constants of inactivation; see exercise 7.

9. **[M.S.]** Modify the MATLAB program from exercise 6 to handle multiple currents.

10. **[M.S.]** Add a PDE solver to the MATLAB program from exercise 6 to simulate poor space and voltage clamp conditions.

11. **[Ph.D.]** Introduce numerical optimization into the dynamic clamp protocol to analyze experimentally in real time the (in)activation parameters of membrane currents.

12. **[Ph.D.]** Use new classification of families of channels (Kv3,1, $Na_v1.2$, etc.; see Hille 2001) to determine the kinetics of each subgroup, and provide a complete table similar to those in section 2.3.5.